Acylation of β-Lactams by Class A β-Lactamase: An *ab Initio* Theoretical Study on the Effects of the Oxy-Anion Hole

Brian D. Wladkowski,* Sarah A. Chenoweth, Julie N. Sanders, Morris Krauss, and Walter J. Stevens*

Contribution from the Department of Chemistry, Western Maryland College, Two College Hill, Westminster, Maryland 21157, and Center for Advanced Research in Biotechnology, National Institute of Standards and Technology, 9600 Gudelsky Drive, Rockville, Maryland 20850

Received October 23, 1996[⊗]

Abstract: The initial acylation step in the β-lactamase catalyzed hydrolysis of β-lactams is studied using an *ab initio* quantum mechanical approach. The computational model incorporates a simple β-lactam substrate and key residues found in the active site in order to assess the plausibility of a specific mechanism originally proposed by Strynadka *et al.*[1] and to estimate the stabilizing effects of the oxy-anion hole components founds in these enzymes. The computational model was constructed using information obtained from a high resolution X-ray crystal structure of unbound native β-lactamase, isolated from *Staphylococcus aureus* PC1. Within this model, the overall acylation reaction was found to occur with modest activation energy <26 kcal mol^{-1} (<109 kJ mol^{-1}) through a microscopic pathway characterized by discrete proton transfer steps between the substrate and the active site residues Ser-70, Lys-73, and Ser-130. These energetic results are considerably lower than the activation energies found for the uncatalyzed hydrolysis of simple amides in the gas phase. Interestingly, the energetic stabilization of the components, which make up the oxy-anion hole, were found to be modest with only one stationary point on the potential energy surface being significantly reduced by ∼8 kcal mol^{-1} (∼33 kJ mol^{-1}).

Introduction

Over the past 40 years β-lactam containing antibiotics, including the penicillins and the cephalosporins, have been the primary pharmaceuticals used to fight bacterial infection. These antibiotics function by killing bacterial cells through an irreversible inhibition of a number of enzymes essential to the synthesis of the cell walls.[2] In recent years, the therapeutic effectiveness of many β-lactam-containing antibiotics has been significantly reduced by the emergence of resistant strains of bacteria which are able to break down these compounds before they can carry out their designed role. These mutant bacteria have developed resistance to common antibiotics primarily through the synthesis of β-lactamase enzymes. Now found in many types of bacteria, β-lactamases constitute a group of bacterial enzymes that destroy clinically useful antibiotics by hydrolyzing the sensitive four-membered β-lactam ring, the active functional group in these compounds.[3] Since they were first discovered, β-lactamases have been the subject of extensive analyses to probe various biophysical properties. A number of high-resolution X-ray crystal structures of the class A β-lactamases, the largest class of these bacterial enzymes, have recently been determined, including those isolated from *Staphylococcus aureus* PC1,[4] *Bacillus licheniformis*,[5] *Streptomyces albus* G,[6] *Bacillus cereus*,[7] and *Escherichia coli*.[8] In addition to the extensive structural work, kinetic studies of the native and mutant systems have revealed a great deal about the overall enzymatic mechanism.[9−14] Through these extensive experimental analyses, it was found that class A β-lactamases are essentially serine hydrolases which function by hydrolyzing the antibiotic through a two-step acylation−hydrolysis pathway shown in Figure 1.

In the first step of the mechanism the substrate undergoes initial attack by an active-site serine residue (Ser-70) at the carbonyl carbon of the sensitive β-lactam ring, forming a covalently bound acyl intermediate. In the subsequent hydrolysis step, a uniquely positioned water molecule within the active site acts as the nucleophile hydrolyzing the acyl intermediate and releasing product. Like the more general serine proteases, class A β-lactamases were also found to contain a conserved

[⊗] Abstract published in *Advance ACS Abstracts,* June 15, 1997.

(1) Strynadka, N. C.; Adachi, H.; Jensen, S. E.; Johns, K.; Sielecki, A.; Betzel, C.; Sutoh, K.; James, M. N. G. *Nature* **1992**, *359*, 700.

(2) Herzberg, O.; Moult, J. *Curr. Opin. Struct. Biol.* **1991**, *1*, 946.

(3) Waley, S. G. In *The Chemistry of β−Lactams*; Page, M. I., Ed.; Chapman & Hall: London, 1992.

(4) (a) Herzberg, O.; Moult, J. *Science* **1987**, *236*, 694. (b) Herzberg, O. *J. Mol. Biol.* **1991**, *217*, 701. (c) Chen. C. C. H.; Rahil, J.; Pratt, R. F.; Herzberg. O. *J. Mol. Biol.* **1993**, *234*, 165. (d) Chen, C. C. H.; Herzberg, O. *J. Mol. Biol.* **1992**, *224*, 1103. (e) Herzberg, O.; Kapadia, G.; Blanco, B.; Smith, T. S.; Coulson, A. *Biochemistry* **1991**, *30*, 9503.

(5) (a) Moews, P. C.; Knox, J. R.; Dideberg, O.; Charlier, P.; Frre, J.-M. *Proteins: Struct. Funct. Genet.* **1990**, *7*, 156. (b) Knox, J. R.; Moews, P. C. *J. Mol. Biol.* **1991**, *220*, 435. (c) Knox, J. R.; Moews, P. C.; Escobar, W. A.; Fink, A. L. *Protein Eng.* **1993**, *6*, 11.

(6) Dideberg, O.; Charlier, P.; Wéry, J. P.; Dehottay, P.; Dusart, J.; Erpicum, T.; Frre, J.-M.; Ghuysen, J.-M. *Biochem. J.* **1987**, *245*, 911.

(7) Samraoni, B.; Sutton, B. J.; Todd, R. J.; Artymiuk, P. J.; Waley, S. G.; Phillips, D. C. *Nature* **1986**, *320*, 378.

(8) (a) Jelsch, C.; Lenfant, F.; Masson, J. M.; Samama, J. P. *FEBS Lett.* **1992**, *299*, 135. (b) Jelsch, C.; Mourey, L.; Masson, J. M.; Samama, J. P. *Proteins: Struct. Funct. Genet.* **1993**, *16*, 364.

(9) (a) Knowles, J. R. *Acc. Chem. Res.* **1985**, *18*, 97. (b) Fisher, J.; Belsaco, J. G.; Khosla, S.; Knowles, J. R. *Biochemistry* **1980**, *19*, 2895.

(10) (a) Christensen, H.; Martin, M. T.; Waley, S. G. *Biochem. J.* **1990**, *266*, 853. (b) Gibson, R. M.; Christensen, H.; Waley, S. G. *Biochem. J.* **1990**, *272*, 613. (c) Martin, M. T.; Waley, S. G. *Biochem. J.* **1988**, *254*, 923.

(11) Adachi, H.; Ohta, T.; Matsuzawa, H. *J. Biol. Chem.* **1991**, *266*, 3186.

(12) (a) Escobar, W. A.; Tan, A. K.; Fink, A. L. *Biochemistry* **1991**, *30*, 10783. (b) Ellerby, L. M.; Escobar, W. A.; Fink, A. L.; Mitchinson, C.; Wells, J. A. *Biochemistry* **1990**, *29*, 5797. (c) Virden, R.; Tan, A. K.; Fink, A. L. *Biochemistry* **1990**, *29*, 145. (d) Cartwright, S. J.; Tan, A. K.; Fink, A. L. *Biochem. J.* **1989**, *263*, 905.

(13) (a) Dalbadie-McFarland, G.; Neitzel, J. J.; Richards, J. H. *Biochemistry* **1986**, *25*, 332. (b) Healey, W. J.; Labgold, M. R.; Richards, J. H. *Proteins Struct. Funct. Genet.* **1989**, *6*, 275.

(14) (a) Jacob, F.; Joris, B.; Dideberg, O.; Dusart, J.; Ghuisen, J.-M.; Frére, J.-M. *Protein Eng.* **1990**, *4*, 79. (b) Jacob, F.; Joris, B.; Lepage, S.; Dusart, J.; Frére, J.-M. *Biochem. J.* **1990**, *271*, 399.

S0002-7863(96)03678-5 CCC: $14.00

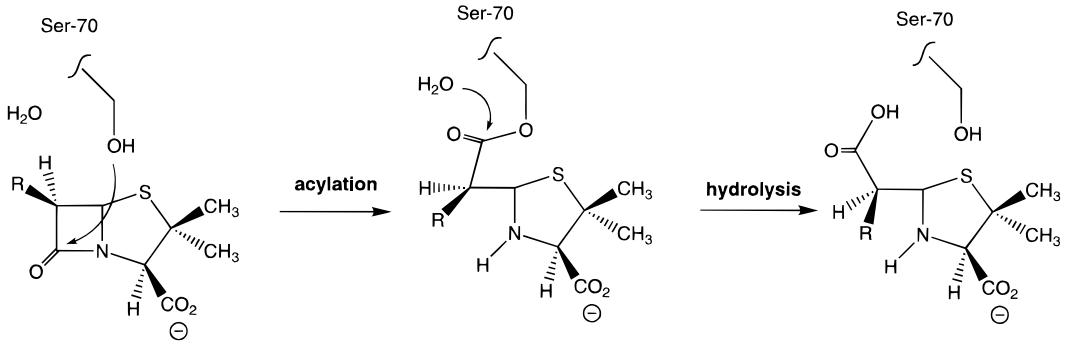

Figure 1. Qualitative mechanism for the overall hydrolysis of β-lactam antibiotics by class A β-lactamase.

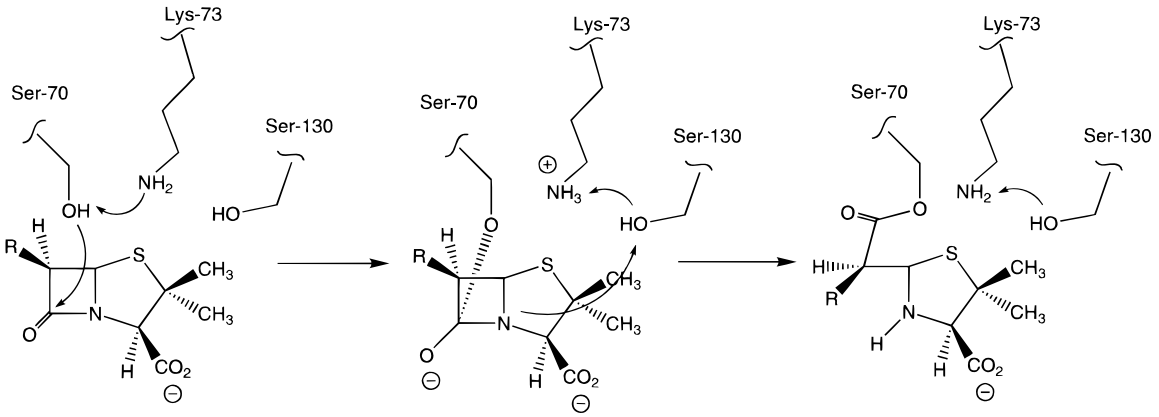

Figure 2. The basic features of the initial acylation mechanism in the overall hydrolysis of β-lactam by β-lactamase proposed by Strynadka *et al*.

structural feature analogous to the "oxy-anion hole". The backbone amide linkages of two active-site residues (Ser-70 and Gln-245 in the case of class A β-lactamase) orient to form a pocket or hole to which the substrate lactam carbonyl oxygen binds.

Although the qualitative features of the overall β-lactamase mechanism illustrated in Figure 1 have been well established, a number of fundamental questions regarding the details of the microscopic mechanism remain unanswered. The most important questions center around the details of the essential proton transfer steps in the acylation mechanism involving the deprotonation of the serine hydroxyl group and protonation of the lactam nitrogen, specifically which active site residues play an active role. Other important questions concerning the β-lactamase microscopic mechanism involve the role of the oxy-anion hole. Recently, Herzberg and Moult summarized several different proposed acylation mechanisms on the basis of their crystallographic results of the native and phosphonate-bound enzyme isolated from *S. aureus* PC1.[2] The first of these mechanisms is based on a direct attack of Ser-70 on the substrate in which the Ser-70 transfers a hydroxyl proton directly to the lactam nitrogen of the substrate as the hydroxyl oxygen attacks the carbonyl carbon. On the basis of this picture, the other conserved active site residues do not play a direct role in the catalytic function for acylation, but merely mediate the direct transfer process. Another proposed mechanism involves Glu-166 as the base which deprotonates the Ser-70 hydroxyl group prior to attack. Although plausible, neither of these two mechanisms has been confirmed. More recently, Strynadka *et al.* proposed a very different and more complicated microscopic mechanism for the acylation step based on crystallographic structures of an unbound native class A β-lactamase isolated from *E. coli* and a covalently bound enzyme-intermediate of an E166N mutant. On the basis of the relative position and orientation of certain active site residues Strynadka *et al.* argued that the proton is transferred *indirectly* from Ser-70 to the lactam nitrogen through a series of steps involving Lys-73 and Ser-130 as shown in Figure 2. The quantum mechanical calculations described in this paper were specifically designed to determine the validity of the above mechanism and include, for the first time, realistic models of the substrate and critical active site residues.

Recently, a number of theoretical studies have appeared that attempt to address some of the more specific details of the microscopic mechanism for the hydrolysis of amide linkages in general.[15−28] Several studies have combined classical mechanics with kinetics studies to investigate various β-lactamase mutations. Juteau *et al.*[15] applied this technique to investigate the role of a specific active-site residue, while Bulychev *et al.*[16] focused on the mechanistic inactivation of several prototypic β-lactamases. Denny *et al.*[17] used this combination again to define the interaction between β-lactamase and a known inhibitor. Molecular mechanics applications have also been used independently to refine structural models previously determined through X-ray crystallography. Boyd and Snoddy[18] utilized gas-phase as well as solvated models to examine the structure of two complete penicillin-recognizing proteins. A more complete gas-phase structure for a class A β-lactamase was similarly determined by Bunster *et al.*,[19] and Vijayakumar[20] employed a solvated model of another class A β-lactamase to pinpoint several significant residues in an analysis of the active site.

Although classical-based molecular modeling techniques can provide valuable structural information regarding various classes

(15) Juteau, J.; Billings, E.; Knox, J. R.; Levesque, R. C. *Protein Eng.* **1992**, *5*, 693.
(16) Bulychev, A.; Massova, I.; Lerner, S. A.; Mobashery, S. *J. Am. Chem. Soc.* **1995**, *117*, 4797.
(17) Denny, B. J.; Toomer, C. A.; Lambert, P. A. *Microbios*. **1994**, *78*, 245.
(18) Boyd, D. B.; Snoddy, J. D. *Mol. Aspects Chemother., Proc. Int. Symp., 3rd*. **1992**, 1.
(19) Bunster, M.; Cid, H.; Canales, M. *Med. Sci. Res*. **1995**, *23*, 751.
(20) Vijayakumar, S.; Ravishanker, G.; Pratt, R. F.; Beveridge, D. L. *J. Am. Chem. Soc*. **1995**, *117*, 1722.

of β-lactamases and related inhibitors, they cannot be used to examine specific intermediate and transition states along the reaction pathway quantitatively or readily treat local ionicity including the movement of protons. Practical time limits imposed by current quantum mechanical techniques when dealing with molecules of this complexity generally has led to the use of small models or the use of hybrid quantum/classical methods to analyze large chemical systems, especially those involving protein structure. Nangia[21] applied such a semiempirical method to determine AM1 heats of formation for the hydrolysis of modified β-lactams, examining a mechanism-based inactivation of existing β-lactamase enzymes. A combination of kinetic and semiempirical techniques has been utilized by Matagne *et al.*[22] to determine the reactivity of several purportedly stable classes of β-lactams when exposed to class A β-lactamases. AM1 energy optimizations have shown various β-lactam variants to have a greater susceptibility to hydrolysis than previously determined. Finally, Warshel *et al.*[23] have completed extensive studies on a number of enzyme-catalyzed reaction mechanisms including the effects of solvation using a mixed quantum/classical approach involving valence bond (VB) theory.

For a complex enzymatic mechanism such as that proposed for β-lactamase it is clear that the most quantitative approach requires quantum mechanical techniques based on models which include the chemically relevant protein residues. Charge transfer processes, which play an essential role in the interaction between the substrate and the active site of the enzyme, must be analyzed explicitly to develop a realistic representation. Although such an approach has been lacking, a number of researchers have used *ab initio* techniques to answer related questions. Fernandez and Van Alsenoy[24] employed a purely *ab initio* model to determine the most favorable conformations of clavulanic acid, a known β-lactamase inhibitor. The energetic trends of additional inhibitors were investigated by Fernandez *et al.*[25] using a similar *ab initio* method. However, neither of these studies incorporated the β-lactam ring or essential parts of the enzyme itself. Investigations into specific features of the reaction pathway utilizing quantum treatments have also been applied to related amide systems including a semiempirical and *ab initio* study by Jensen *et al.*[26] to analyze stepwise and concerted mechanisms for the formation of a peptide bond between molecules of glycine. An examination of the water-assisted hydrolysis of a peptide bond similar to that found in the β-lactam ring was also undertaken by Antonczak *et al.*[27] at the *ab initio* level. The formamide molecule was used as a simple representative of peptide bonds found in many systems of biological importance. The most relevant theoretical work to date on the β-lactamase catalysis has been carried out by Wolf *et al.*[28] Using both semiempirical and *ab initio* quantum techniques, the alcoholysis pathway of several simple β-lactams was studied including the important transition-state structures. Interestingly, a significant reduction in the activation energy for the water-assisted reaction was found. Despite these individual successes, a more complete understanding of the complex β-lactamase mechanism cannot be achieved through such models, and can only be obtained from an analysis of the specific components involved in interactions between the enzyme and substrate.

An important long-term research goal related to the study of β-lactamases is to circumvent these evolutionary enzymes through the development of novel non-β-lactam antibiotics which kill bacteria cells through alternate routes. A more direct, and perhaps more fruitful, short-term approach would be to design modified β-lactam antibiotics or design β-lactamase inhibitors to increase the effectiveness of currently available drugs. It has become clear from the studies undertaken thus far that, in order to do so, the details surrounding the complex microscopic enzymatic mechanism by which β-lactamases function must be resolved.

Recently, we developed a quantum mechanical approach for studying enzyme catalyzed reaction mechanisms and successfully applied it to the transphosphorylation step in the enzyme catalyzed hydrolysis of phosphodiester by ribonuclease A.[29] In the present investigation we explore the acylation step in the β-lactamase catalyzed hydrolysis of β-lactams using a similar *ab initio* quantum mechanical approach. The model used here incorporates a simple substrate and key active-site residue components and is based on information obtained from a high-resolution X-ray crystal structure of the unbound native β-lactamase, isolated from *S. aureus* PC1.[2] Our goal is to examine the plausibility of the novel mechanism proposed recently by Strynadka *et al.*[1] by characterizing the microscopic mechanism computationally using a model which incorporates the necessary components of the mechanism. Particular emphasis is placed on the individual proton-transfer steps that occur between the substrate and the active-site residues. A secondary goal of this work is to examine the role of the "oxy-anion hole", an essential feature of serine proteases involving backbone amide linkages, thought to stabilize the developing negative charge on the substrate carbonyl oxygen as the substrate undergoes nucleophilic attack by Ser-70. This latter goal will be accomplished by probing critical structural features along the enzyme-catalyzed reaction pathway using computational models with and without the oxy-anion hole components.

The next section contains a detailed description of the computational models used to map out the reaction surface, including the components in the model, the constraints imposed, and the calculational details. In Results and Discussion, the structural and energetic results are presented and discussed in the context of available experimental data. Finally, the results are summarized in the final section.

Theoretical Model

Basic Features. Two different all-electron quantum mechanical models were used in this investigation to explore the structural and energetic features of the acylation step in the overall enzyme-catalyzed hydrolysis of β-lactams by class A β-lactamases. The two models differ only in the components which make up the oxy-anion hole as a means to assess the importance of these components in stabilizing key features along the reaction pathway. Due to size limitations inherent in the Hartree−Fock and correlated *ab initio* methods, the total number of atoms included in the all-electron models must be restricted, and therefore, careful choice of the components which make

(21) Nangia, A. *Proc. - Indian Acad. Sci., Chem. Sci*. **1993**, *105*, 131.
(22) (a) Matagne, A.; Misselyn-Bauduin, A.; Joris, B.; Erpicum, T.; Granier, B.; Frere, J. *Biochem. J*. **1990**, *265*, 131. (b) Matagne, A.; Lamotte-Brasseur, J.; Dive, G.; Knox, J. R.; Frere, J. *Biochem. J*. **1993**, *293*, 607. (c) Matagne, A.; Lamotte-Brasseur, J.; Frere, J. *Eur. J. Biochem*. **1993**, *217*, 61.
(23) Warshel, A.; Levitt, M. *J. Mol. Biol*. **1976**, *103*, 227.
(24) Fernandez, B.; Van Alsenoy, C. *Struct, Chem*. **1992**, *3*, 321.
(25) Fernandez, B.; Carballeira, L.; Rios, M. A. *Biopolymers* **1992**, *32*, 97.
(26) Jensen, J. H.; Baldridge, K. K.; Gordon, M. S. *J. Phys. Chem*. **1992**, *96*, 8340.
(27) Antonczak, S.; Ruiz-Lopez, M. F.; Rivail, J. L. *J. Am. Chem. Soc*. **1994**, *116*, 3912.
(28) (a) Wolfe, S. *Can. J. Chem*. **1994**, *72*, 1014. (b) Wolfe, S. *Can. J. Chem*. **1994**, *72*, 1033. (c) Wolfe, S. *Can. J. Chem*. **1994**, *72*, 1044. (d) Wolfe, S. *Can. J. Chem*. **1994**, *72*, 1066.
(29) (a) Wladkowski, B. D.; Krauss, M.; Stevens, W. J. *J. Phys. Chem.* **1995**, *99*, 6273. (b) Wladkowski, B. D.; Krauss, M.; Stevens, W. J. *J. Am. Chem. Soc.* **1995**, *117*, 10537.

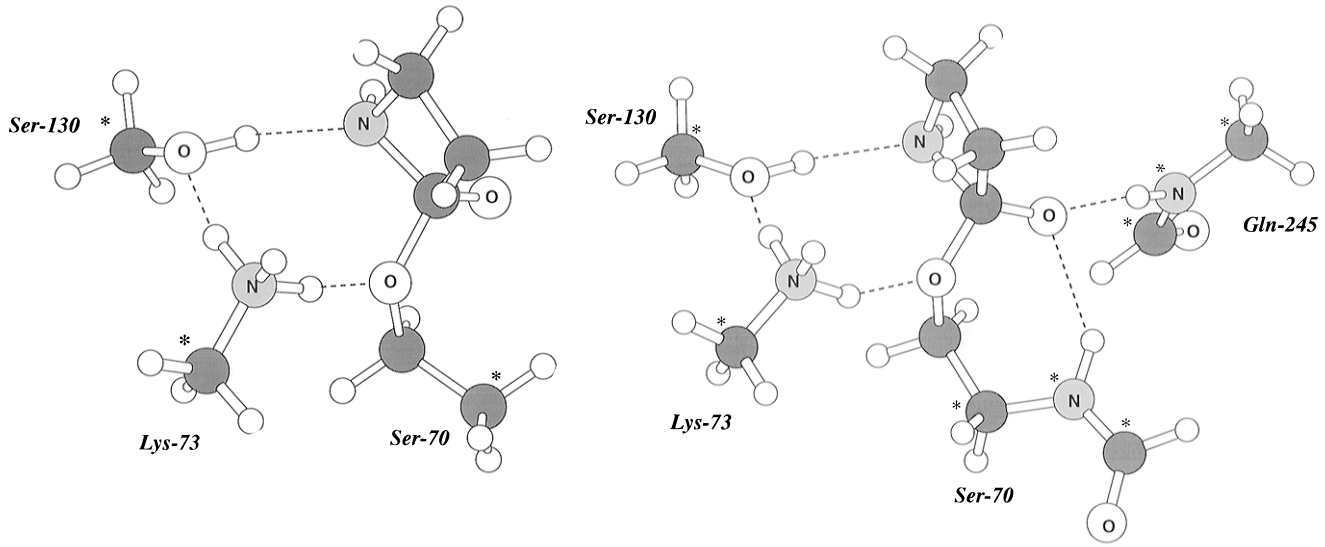

Figure 3. All-electron quantum mechanical model used to map out the acylation step in β-lactamase catalysis: (a, left) without the oxy-anion hole backbone amide linkage and (b, right) with the oxy-anion hole backbone amide linkage. Atoms marked with an asterisk (*) were held fixed to their positions found crystallographically.

up the active site must be made. Each model contains several parts, including a simple β-lactam substrate, propiolactam, and essential *pieces* of key amino acid residues found in the β-lactamase active site. For both models, propiolactam was chosen as the prototype substrate because it represents the smallest β-lactam appropriate for the enzyme-catalyzed acylation reaction of interest. In addition to the substrate, model 1 contains side chains of the essential Ser-70, Lys-73, and Ser-130 residues. Model 2 contains, in addition to the components in Model 1, the backbone atoms of Ser-70 and Gln-245, which make up the oxy-anion hole components. Shown in parts a and b of Figure 3 are three-dimensional representations of the two computational models at an intermediate stage along the acylation reaction pathway to help illustrate the differences between the models and the spatial arrangement of the atoms in the active site. For several of the active-site amino acids mentioned above, the complete side chains are too large to be included in the all-electron models directly. As a result, certain residues are represented by small molecular subunits designed to mimic the important features of each. As seen in Figure 3a,b, the complete Ser-73 residue is used including the backbone amide linkage. However, a methylamine is used to represent Lys-71, methanol is used to represent Ser-130, and a formamide molecule is used to represent the backbone of Gln-245. These so called "pseudoresidues" (hereafter written in italic to distinguish them from the complete residue) are designed to encompass the necessary electronic framework and allow for electron rearrangement, including possible proton transfer, between important active site components and the substrate while maintaining a tractable size all-electron system to probe energetics quantitatively.

Constraints. In order to develop computational models which are appropriate for assessing features of the enzyme catalyzed reaction pathway, certain constraints due to the protein structural framework must be imposed on the basis of experimental information of the actual enzyme active site. Such constraints are critical to the development of a physically meaningful model by preventing movement of certain atoms, or groups of atoms, to unrealistic relative positions unattainable in the actual system. Imposing too many constraints, however, can also be detrimental in that a highly rigid model may not have sufficient sidechain mobility to achieve optimal atomic arrangements for reaction. The X-ray structure of the covalently bound acyl−enzyme intermediate complex obtained by Strynadka *et al.*[1] would be the most appropriate structure upon which to base the necessary constraints. However, the coordinates have not been made available to the scientific community. As a result, for this investigation, the structure obtained from high-resolution X-ray crystallographic data of the class A β-lactamase isolated from *S. aureus* PC1, obtained by Herzberg *et al.*,[2] was used as a reference. A partial three-dimensional representation of the β-lactamase active site obtained directly from the Herzberg X-ray structure refinement, with the superimposed, geometry-optimized quantum mechanical model, is given in Figure 4 and illustrates the relative position of all non-hydrogen atoms from each residue in the active site. The heavy atoms, identified with an asterisk in the computational models shown in Figure 3a,b, were held fixed throughout the computations in the same absolute positions found in the refined X-ray structure. It is important to point out, however, that no other atoms, including those of the β-lactam substrate, were held fixed, and no additional internal constraints were imposed on the quantum system. Constructing the quantum mechanical models in this way resulted in highly flexible systems with 81 and 105 internal degrees of freedom for models 1 and 2, respectively.

Protonation State. The overall protonation state of the system used here is based on the fundamental mechanism of β-lactamase catalysis proposed by Strynadka *et al.*[1] illustrated in Figure 2. The critical feature of this mechanism requires Lys-73 to be deprotonated once the substrate binds, resulting in an overall neutral quantum mechanical model as illustrated in Figure 3a,b. Other reaction mechanisms with other active-site protonation states have been proposed but are not studied here. Strynadka *et al.*[1] have argued that the pK_a of Lys-73 is unusually low, and therefore, it exists in its neutral form initially because of its close proximity to other highly charged residues including Glu-166 and Lys-234. It should be pointed out, however, that results obtained by Damblon *et al.*[30] based on NMR analysis of the unligated enzyme, imply that Lys-73 is protonated initially and therefore cannot act as a general base in the initial step of the enzymatic mechanism. Also, recent X-ray crystallographic analysis of an unbound K73H β-lactamase mutant by Herzberg *et al.*[31] shows that the His-73 appears

(30) Damblon, C.; Raquet, X.; Lian, L-Y.; Lamotte-Brasseur, J.; Fonze, E.; Charlier, P.; Roberts, G. C. K.; Frére, J-M. *Proc. Natl. Acad. Sci. U.S.A.* **1996**, *93*, 1747.

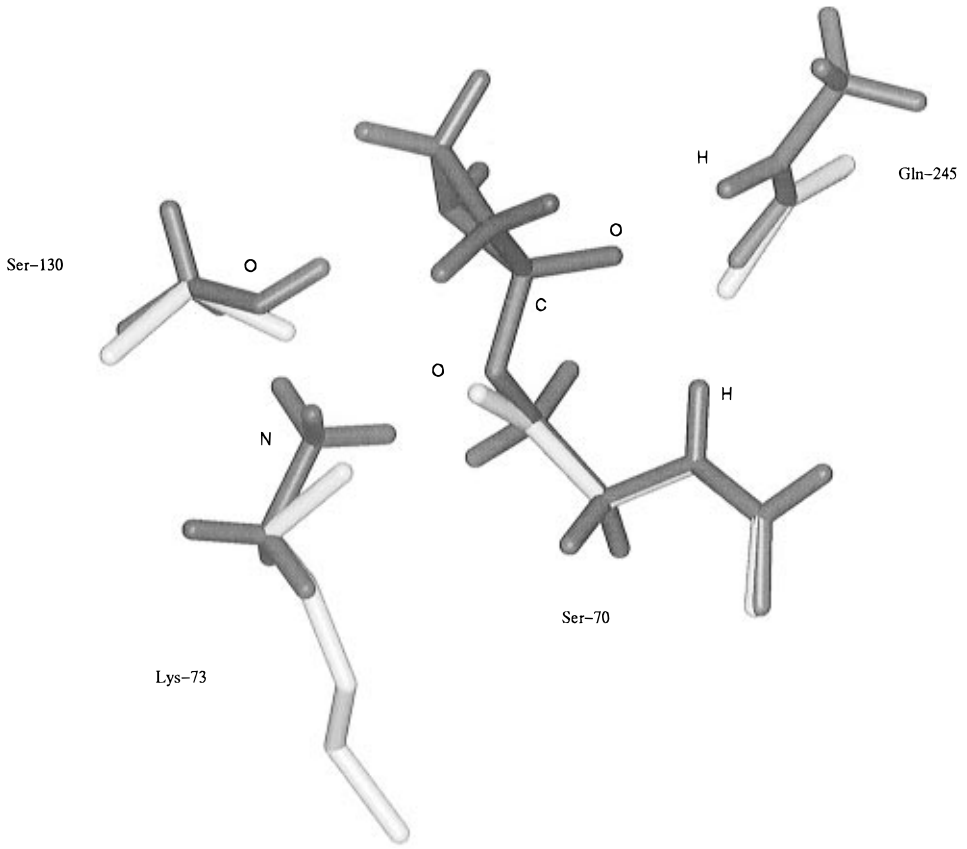

Figure 4. Three-dimensional representation of the β-lactamase active site including the critical residues involved in catalysis obtained directly from the X-ray refinement (lighter bonds) with the optimized quantum model superimposed on top (darker bonds).

to be protonated, suggesting that Lys-73 in the wildtype should also be protonated. By contrast, recent work by Swarén *et al.*[32] on TEM1 β-lactamase using a Poisson−Boltzmann electrostatic analysis showed that the pK_a of Lys-73 is initially 8 and rises to 14 as substrate binds. These results suggest that in fact Lys-73 is significantly deprotonated initially and, moreover, that binding of substrate can alter its pK_a sufficiently for it to act as a general base and deprotonate the Ser-70 hydroxyl group. The protonation state of an actual substrate penicillin or ampicillin molecule may or may not be neutral given the additional functionality of these molecules. It is also assumed here, on the basis of the fundamental mechanism, that the additional features of the natural substrates not included in the present model are important primarily in binding of the substrate to the active site in the correct orientation. This aspect of the overall biochemical function of β-lactamase is not considered here, and therefore, the additional framework of the substrate and enzyme active site are not included. The models constructed here also assume the substrate is bound in the correct orientation to initiate the acylation step.

Theoretical Methods. The atomic-orbital basis sets employed in this study are the standard split valence basis sets of Pople *et al.*[33] designated 3-21G(d) and 6-31+G(d) and are comprised of 148 and 268 contracted Gaussian functions, respectively, for model 1, and 223 and 413 contracted Gaussian functions, respectively, for model 2. Reference electronic wave functions were determined in this investigation by the single-configuration, self-consistent-field, restricted Hartree−Fock method (RHF).[33] The effects of dynamical electron correlation were probed by single point calculations using two methods, second-order Møller−Plesset[33] perturbation theory (MP2) and density functional theory (DFT) using the Becke, Lee, Yang, and Parr (BLYP) correlation and exchange functionals.[34] The electronic structure computations were performed using the GAUSSIAN94 package.[35]

Analytic gradient techniques[33] for the RHF methods were used to perform complete geometry optimizations in internal coordinate space within the Cartesian constraints mentioned above. The lactam substrate was positioned initially according to the model of Herzberg *et al.*,[2] and then was allowed to move freely during the geometry optimization. Its optimum position is determined by interactions with the side chains in the active site, and the carbonyl group remains poised for nucleophilic attack by Ser-70. Quadratic force fields were evaluated via analytic second-derivative techniques for RHF wave functions to aid in the search for minima and transition states. Once located, the complete Hessian was calculated for each stationary point found on the potential energy surface to characterize the extrema as minima or transition states, within the constraints imposed, and to obtain the necessary vibration frequencies used in the standard statistical thermodynamic analysis in calculating ΔG°_{298}. The stationary points along the reaction were located using chemical intuition by first locating plausible

(31) Chen, C. C.; Smith, T. J.; Kapadia, G.; Wäsch, S.; Zawadzke, L. E.; Coulson, A.; Herzberg, O. *Biochemistry* **1996**, *35*, 12251.

(32) Swarén, P.; Maveyraud, L.; Guillet, V.; Masson, J.-M.; Mourey, L.; Samama, J.-P. *Structure* **1995**, *3*, 603.

(33) Hehre, W. J.; Radom, L.; Schleyer, P. v. R.; Pople, J. A. *Ab Initio Molecular Orbital Theory*; Wiley-Interscience: New York, 1986.

(34) (a) Becke, A. D. *Phys. Rev.* **1988**, *38*, 3098. (b) Lee, C.; Yang, W.; Parr, R. G. *Phys. Rev. B* **1988**, *37*, 78. (c) Miehlich, B.; Savin, A.; Stoll, H.; Preuss, H. *Chem. Phys. Lett.* **1989**, *157*, 200.

(35) All computations were performed on IBM RS/6000 workstations or a CRAY J90 running Gaussian 94 package: Frisch, M. J.; Trucks, G. W.; Head-Gordon, M.; Gill, P. M. W.; Wong, M. W.; Foresman, J. B.; Johnson, B. G.; Schlegel, H. B.; Robb, M. A.; Replogle, E. S.; Gomperts, R.; Andres, J. L.; Raghavachari, K.; Binkley, J. S.; Gonzalez, C.; Martin, R. L.; Fox, D. J.; Defrees, D. J.; Baker, J.; Stewart, J. J. P.; Pople, J. A. *Gaussian 94*, Revision A; Gaussian, Inc., Pittsburgh PA, 1994.

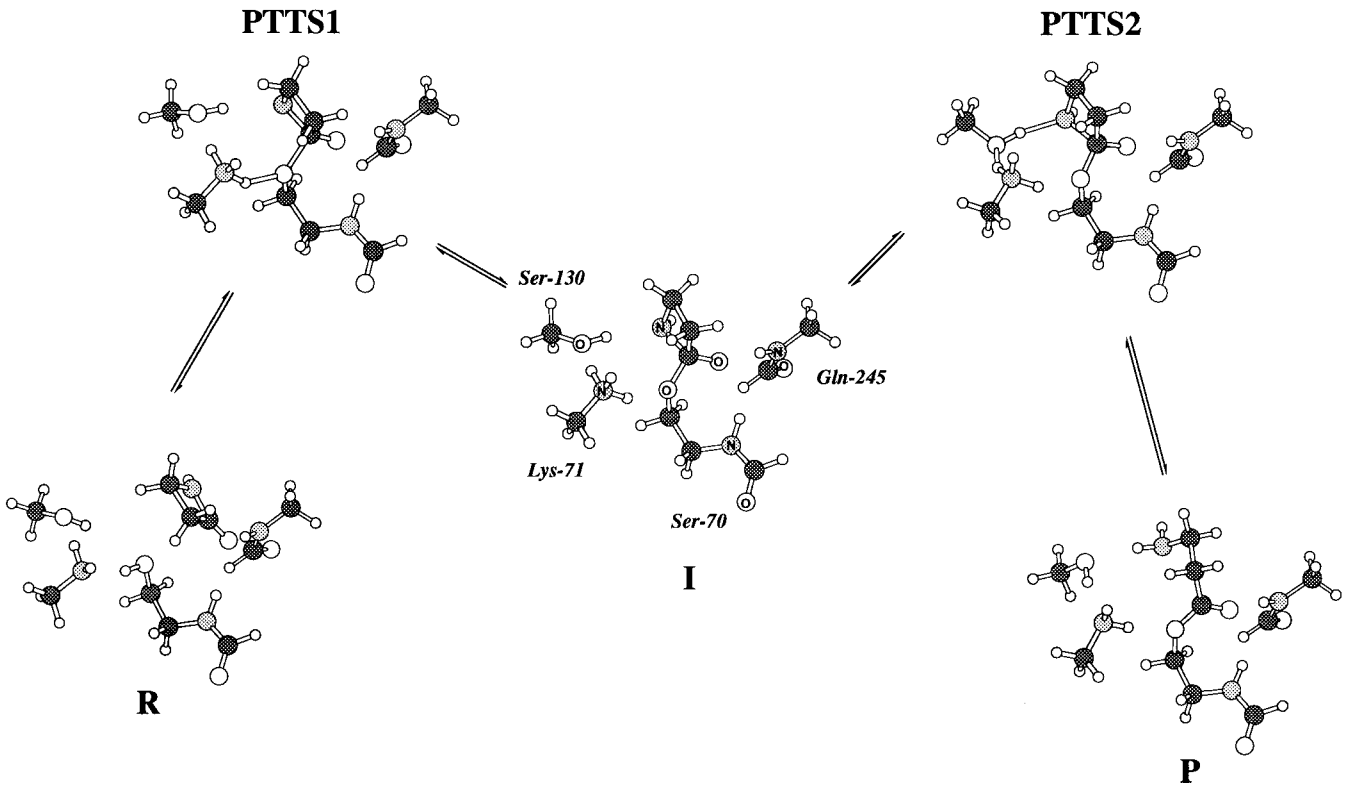

Figure 5. Stationary structures located along the acylation reaction pathway determined at the RHF/6-31+G(d) level (see text).

intermediates consistent with the overall chemical reaction. Transition states, connecting the intermediates to both the reactant and product state, were then located using standard reaction coordinate following techniques. It should be made clear, however, that although the microscopic mechanisms presented here for the two models are continuous reaction pathways a complete search was not done, and other reaction pathways of lower energy, which connect the reactant and product states, may exist.

Finally, to better understand the effects of electron correlation on the geometry of the stationary points along the reaction surface, DFT optimization using the BLYP functionals were carried out on the minimum structure. Correlated transition state structures, however, could not be obtained.

Results and Discussion

Microscopic Reaction Mechanism. Figure 5 shows three-dimensional representations of the five stationary points (three minima and two transition states) found along the acylation pathway connecting the bound reactant and product complexes based on the more complete model 2. The qualitative features of the acylation pathway for model 1 were essentially identical, containing three minima and two transition states. The results shown are the optimized structures obtained at the RHF level using the larger 6-31+G(d) basis set.

As with other serine proteases, the initial step in the overall β-lactamase mechanism involves nucleophilic attack of an active site serine hydroxyl group on the substrate β-lactam carbonyl carbon to form the acyl enzyme intermediate. As seen in Figure 5, the basic features of this mechanism are borne out in the computational results based on the simplified models described above. Propagation along the reaction coordinate from the reactant complex, **R**, to the product complex, **P**, leads to a contraction of the Ser-70 O^{γ} oxygen to substrate carbonyl carbon bond distance from 2.954 to 1.316 Å at the RHF/6-31+G(d) level. Although, qualitatively, this reaction can be considered simple acylation at an sp_2-hybridized carbon, the microscopic mechanism must involve several proton transfer steps. At a minimum, the Ser-70 hydroxyl group must be deprotonated and the substrate amide nitrogen must be protonated. Conceptually, the most straightforward means of accomplishing this is through a direct proton transfer between these two heteroatoms. As mentioned above, a direct attack mechanism has been discussed by Herzberg *et al.*[2] on the basis of crystallographic data for both the native enzyme (*S. aureus* PC1) and various analog bound systems. However, preliminary computational results, not reported here, suggest that such a direct attack mechanism would require a substantial activation energy due to a highly strained transition state. Instead, our calculations support the plausibility of the reaction mechanism originally proposed by Strynadka *et al.*[1] in which the enzyme, utilizing its active-site framework to provide additional sites with comparable proton affinities, allows the proton to be removed from the nucleophile and added to the leaving group in a sequence of indirect steps, each of which is less energetically costly, and hence more facile than a direct transfer. Inclusion of the Lys-73 and Ser-130 pseudoresidues into the computational model provides these necessary sites and allows the essential proton transfers to occur in two steps.

Within the current computational model, starting with the bound reactant complex, **R**, the most energetically accessible reaction pathway involves an initial proton transfer between Ser-70 O^{γ} and Lys-73 N^{ζ}. Once past this proton transfer transition state, **PTTS1**, the system forms a metastable oxy-anion intermediate state, **I**, in which the acyl bond is partially formed and the carbonyl carbon of the substrate is tetravalent. It is at this stage, where the developing negative charge on the carbonyl oxygen is maximized, that the backbone amide components of the active site (the oxy-anion hole) exhibit their most stabilizing influence. Once formed, this metastable intermediate can go on to form product through a concerted step which involves simultaneous (1) proton transfer from the Lys-73 N^{ζ} to Ser-130 O^{γ}, (2) proton transfer from Ser-130 O^{γ} to the substrate amide nitrogen, and (3) cleavage of the β-lactam amide bond.

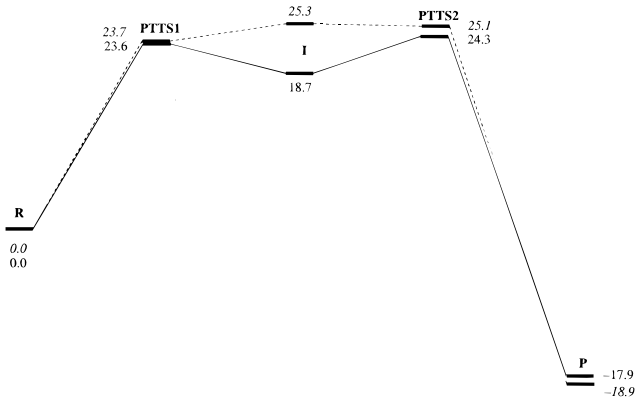

Figure 6. Relative electronic energy diagram (ΔE_e°, kcal mol^{-1}; 1 kcal mol^{-1} = 4.184 kJ mol^{-1}) for the stationary points located along the acylation pathway at the MP2/6-31+G(d)//RHF/6-31+(d) level: (—, Roman type) with and (- - -, italic type) without oxy-anion hole (*Gln245*, Ser70).

Although this sequence of events occurs through a concerted step in the model developed here, at other levels of theory, these may in fact be discrete steps in the actual enzyme reaction mechanism. Here, only a single transition state was identified, **PTTS2**. Once past this second proton-transfer transition state, the acyl enzyme intermediate complex, **P**, is formed directly.

There are a number of interesting structural features of the model system at the different stages along the reaction path worth mentioning. First, although not obvious from the position of active-site residues obtained crystallographically, a structural network is set up to allow proton transfers to occur in an in-line fashion between pairs of heteroatoms. As shown in Figure 3a,b, a five-membered ring pattern exists, consisting of the substrate amide linkage (C and N), nucleophilic Ser-70 O$^\gamma$, Lys-73 N$^\zeta$, and Ser-130 O$^\gamma$. The adjacent heteroatom distances in the intermediate structure, **I**, range from 1.458 to 2.947 Å at the RHF level. This network insures that no single proton must be transferred over a large distance or in a nonlinear fashion. It is also interesting to point out that this network did not originally exist in the X-ray crystal structure of the unbound native enzyme but resulted from optimization of the model. In fact, the position of Lys-73 N$^\zeta$ moves nearly 1 Å to its position in the current model. This movement of key herteroatoms to set up a proton transfer network, clearly evident from Figure 4, is consistent with the limited structural information reported by Strynadka *et al.*[1] There are many possible reasons for this change in structure. The neutral lysine side chain is very mobile and its movement upon substrate binding may be part of its designed role. Also, Glu-166 which exists adjacent to Lys-73 in the active site is not included in the computational model. Therefore, any attractive interaction between these two residues which exists in the real system is not accounted for in the present model.

Another interesting structural feature of the computational model at the intermediate stage **I** is the orientation of the oxy-anion hole backbone amide protons. As can be seen in Figure 3b, while the *Gln-245* NH is oriented directly toward the carbonyl oxygen of the substrate, the NH from Ser-70 is displaced considerably from linearity. The *Gln-245* and Ser-70 amide nitrogen to carbonyl oxygen distance are however, quite similar, 3.061 and 3.000 Å, respectively. It appears that the backbone amide linkages are able to stabilize the developing negative charge without being directly oriented.

Electronic Energy Surface. Figure 6 shows a graphical representation of the intrinsic electronic energy surface, ΔE_e°, for both models 1 and 2 at the highest quantum mechanical level used, MP2/6-31+G(d)//RHF/6-31+G(d), highlighting the influence of the oxy-anion hole components on the surface energetics. The complete list of relative energetic data for each stationary point from both model systems at the RHF, BLYP, and MP2 level are also given in Table 1, illustrating the influence of both basis set augmentation and electron correlation on the electronic energy surface.

Considering the data in Table 1 and the visual representation of the electronic energy surface given in Figures 6, a number of important observations can be made regarding the relative energetics. First, the overall acylation step is highly exothermic [ΔE_e°(P-R) ≈ -18 kcal mol^{-1} (-75 kJ mol^{-1})] for both theoretical models. The BLYP method gives a lower estimate for the reaction energy by 4−5 kcal mol^{-1} (16−20 kJ mol^{-1}) compared to the other levels of theory. As expected, the oxy-anion hole components in the model have little effect on the overall reaction energy as indicated by the similar relative energy of structure **P** for both models. The stabilizing influence of these components on the lactam carbonyl oxygen in the reactants, **R**, is apparently offset by the same interactions with the ester carbonyl oxygen in the product structure **P**. Reaction energies of close to -18 kcal mol^{-1} (-75 kJ mol^{-1}) found here for the acylation step are considerably larger than the reaction energies of -3 to -5 kcal mol^{-1} (-12.5 to -20.9 kJ mol^{-1}) found by Jensen *et al.*[25] for the hydrolysis of simple peptides and dipeptides in the gas phase. Presumably, the additional energy comes from the release in ring strain energy from opening of the four-membered lactam ring which does not exist in simple peptides. Aside from the underestimation at the BLYP level, the overall reaction energy is relatively insensitive to level of theory with variations of less than 2 kcal mol^{-1} (8 kJ mol^{-1}) over the range RHF/3-21G to MP2/6-31+G(d) as seen in Table 1.

Secondly, the overall activation energy for the acylation step was found to be less than 26 kcal mol^{-1} (<109 kJ mol^{-1}) at the highest level of theory used, MP2/6-31+G(d)//RHF/6-31+G(d). The relative energies of both proton transfer transition states (**PTTS1** and **PTTS2**) are very similar and are nearly identical whether the oxy-anion hole components are present or not. Again, these activation energies can be compared to those found for the gas-phase hydrolysis of simple amides by Jensen *et al.*[26] Depending on the reaction pathway and the substrate, activation energies ranging from 40 to 70 kcal mol^{-1} (167 to 293 kJ mol^{-1}) were found. It is clear from these observations that the presence of the active site pseudoresidues in the computational model significantly lowers the overall activation energy for reaction. Moreover, the activation energies are lowered by allowing critical proton transfer steps to occur through a series of in-line processes between the substrate and the active site component heteroatoms. Unlike the relative energy of the product state, **P**, the relative energy of the proton-transfer transition states, and to some extent the intermediate state **I**, are extremely sensitive to level of theory. As seen in Table 1, relative energy differences vary by as much as 35 kcal mol^{-1} (146 kJ mol^{-1}) between RHF/3-21G and MP2/6-31+G* level for these three stationary points. As a result, one must place judicious uncertainties on the final results for these points along the potential energy surface. Part of the observed difference between the RHF and correlated relative energetics could be a result of the effect of electron correlation on the geometric structure of each stationary point since the all correlated calculations were carried out at the RHF geometries. We were able to carry out complete optimizations (within the constraints mentioned above) of the intermediate point **I** on the surface at the BLYP level by using the larger 6-31+G(d) basis set. The relative energy was found to 22.8 kcal mol^{-1} (95.4 kJ mol^{-1}) which compares reasonably well with the BLYP single

Table 1. Relative Energetics, ΔE_e° (kcal mol^{-1}) and ΔG_{298}° (kcal mol^{-1}) for the Stationary Points along the Acylation Reaction Pathway for a Prototype β-Lactam at Various Levels of Theory[b,c]

	3-21G RHF		6-31+G(d) RHF		6-31+G(d)[a] BLYP		6-31+G(d)[a] MP2(fc)	
stationary point	ΔE_e°	ΔG_{298}°	ΔE_e°	ΔG_{298}°	ΔE_e°	ΔG_{298}°	ΔE_e°	ΔG_{298}°
R								
with oxyanion hole	0.0	0.0	0.0	0.0	0.0	0.0	0.0	0.0
(without oxyanion hole)	*(0.0)*	*(0.0)*	*(0.0)*	*(0.0)*	*(0.0)*	*(0.0)*	*(0.0)*	*(0.0)*
PTTS1								
with oxyanion hole	24.9	24.8	44.9	44.8	25.9	25.8	23.6	23.5
(without oxyanion hole)	*(26.9)*	*(36.0)*	*(50.0)*	*(59.1)*	*(30.0)*	*(39.1)*	*(23.7)*	*(32.8)*
I								
with oxyanion hole	18.9	27.2	35.9	44.2	27.4	35.7	18.7	27.0
(without oxyanion hole)	*(25.7)*	*(37.9)*	*(47.7)*	*(59.9)*	*(34.2)*	*(46.4)*	*(25.3)*	*(37.5)*
PTTS2								
with oxyanion hole	19.8	18.9	48.1	47.2	29.2	28.3	24.3	23.4
(without oxyanion hole)	*(25.7)*	*(31.3)*	*(59.0)*	*(64.6)*	*(32.8)*	*(38.4)*	*(25.1)*	*(30.7)*
P								
with oxyanion hole	−18.6	−12.7	−20.9	−15.0	−14.3	−8.3	−17.9	−12.0
(without oxyanion hole)	*(−18.3)*	*(−9.6)*	*(−20.1)*	*(−11.4)*	*(−14.5)*	*(−5.8)*	*(−18.9)*	*(−10.2)*

[a] Single-point calculations at the RHF/6-31+G(d) level of theory. [b] ΔG_{298}°, including zero-point vibrational energy corrections, were determined on the basis of a thermodynamic analysis using harmonic frequencies obtained at the RHF/6-31+G(d) level. [c] 1 kcal mol^{-1} = 4.184 kJ mol^{-1}.

point calculations listed in the table (27.4 kcal mol^{-1}) and suggests that the structural correlation effects are modest.

The most striking feature of the electronic energy surfaces shown in Figure 6 is the stabilizing influence of the oxy-anion hole components on the intermediate state **I** relative to other points on the surface. As seen in the figure, the presence of *Gln-245* and Ser-70 backbone amide linkages has little influence on most of the electronic energy surface. The relative energy of the proton transfer transition states, **PTTS1** and **PTTS2**, as well as the product state, **P**, are shifted by less than 1 kcal mol^{-1} (4 kJ mol^{-1}) at the MP2/6-31+G(d) level. By contrast, the metastable intermediate state, **I**, is stabilized by nearly 7 kcal mol^{-1} (29 kJ mol^{-1}) at the same level of theory due to the presence of these active site components. As expected, the greatest buildup of electron density on the substrate carbonyl oxygen occurs at the intermediate **I** and little additional electron density exists at **PTTS1** and **PTTS2** or **P** relative to that which exists for the reactant state **R**. Consequently, the largest effect of the oxy-anion hole cannot be to reduce the rate-limiting energetic barrier to reaction as is commonly assumed. Although the influence is insignificant for structure **I**, the backbone amide linkages which make up the oxy-anion hole provide only a modest contribution to the overall stabilization of the potential energy surface for the acylation step. It is possible that the primary role of these active-site components is not stabilization of proton-transfer transition states but binding of the substrate and possibly to help maintain the correct orientation of the substrate in the active site. Further studies which address this issue and others related to the hydrolysis step are currently underway.

Thermodynamic Corrections. Also given in Table 1 are estimates of the relative free energies at 298 K, ΔG_{298}°, for each of the stationary points found on the acylation reaction surface for models 1 and 2. The ΔG_{298}° were obtained from a standard statistical thermodynamic analysis based on the harmonic oscillator approximation. The actual values were obtained from corrections to the relative electronic energies discussed above and include zero-point-vibrational (ZPV) corrections, thermal corrections to 298 K, and entropic corrections, based on vibrational frequencies determined at the RHF/6-31+G(d) level. Shown in Figure 7 is a graphical representation of the ΔG_{298}° surface for models 1 and 2.

As can be seen from the figure, the dominant effect of these thermodynamic corrections is to raise the energy of the intermediate state, **I**, relative to the proton-transfer transition

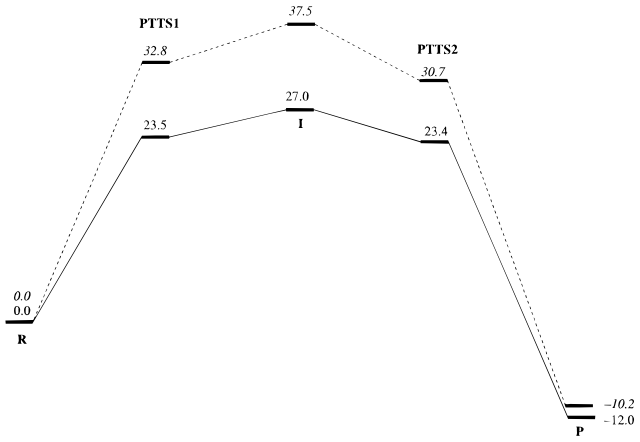

Figure 7. Relative free energy diagram (ΔG_{298}°, kcal mol^{-1}; 1 kcal mol^{-1} = 4.184 kJ mol^{-1}) for the stationary points located along the acylation pathway at the MP2/6-31+G(d)//RHF/6-31+(d) level: (—, Roman type) with and (- - -, italic type) without oxy-anion hole (*Gln245*, Ser70).

states (**PTTS1** and **PTTS2**), resulting in an overall free energy surface where the intermediate state is now the bottleneck to reaction. Moreover, model 1, which does not contain the oxy-anion hole components (Gln-245 and Ser-70 backbones) is more influenced than the more complete Model 2. Although all three thermodynamic terms mentioned above contribute to the shift in relative electronic energy surface, the dominant correction term in ΔG_{298}° is the entropic $T\Delta S$ term. Moreover, this entropic term is dominated by the vibrational entropy in which the lowest vibrational frequencies contribute the most. The apparent shift in the intermediate state free energy compared to the electronic energy surface is consistent with an increase in these low vibrational frequencies as the intermediate is formed. In the reactant state, **R**, there exist a number of very low frequency modes associated with nonbonded torsional and bending modes which shift to much higher frequencies in the intermediate state where the modes have more covalent bonding character. In essence, the intermediate state **I** is a much "tighter" state than the reactant or product states. The relative free energy of the product state is also influenced by these thermodynamic factors, but to a lesser extent. As can be seen, the overall acylation reaction is still highly exergonic, regardless of the model. Therefore, to the extent that the harmonic oscillator model provides a reasonable estimate of the entropic contribution to the free energy surface, it seems possible that the oxy-anion

hole components may still play a role in directly lowering the overall energy barrier to acylation of β-lactams through entropic effects.

The results given in Figure 7 and the associated discussion given above should only be considered qualitatively. It is well known that serious problems can arise in a statistical thermodynamic analysis based on the harmonic oscillator approximation when the system of interest contains many low-vibrational frequencies, as is the case here where as many as 12 vibrational frequencies fall below 200 cm^{-1}. In such cases, the associated low-frequency motions may be hindered rotations or extremely anharmonic vibrations, resulting in serious error in the statistical analysis. At present, there is no easy way to probe the effects of these problems in the current system.

Solvation Effects. Another important factor which can affect enzyme-catalyzed reaction mechanisms, as well as the relative energetics of the intermediates and transition states along the reaction pathway, is solvation. Despite the extensive work[23] to better understand its effects, the role solvent plays in mediating such reactions is by no means clear. In many enzymes, including the β-lactamase system discussed here, the active site, where much of the chemistry takes place, is partially exposed to solvent, but is also surrounded by a significant amount of protein framework. This mixed environment is, to say the least, difficult to model computationally. Ideally, the two different environmental components would be handled individually; the protein environment would be accounted for through specific directional potentials, while the bulk solvent would be handled through some type of solvent continuum.

Although such an approach is not yet available for *ab initio* quantum mechanical applications, the qualitative effects of solvation on enzyme reaction energy surfaces can be gauged using a continuum solvation model alone. In this case, the self-consistent isodensity polarizable continuum model (SCIPCM), developed by Tomasi *et al.*,[35] was used to asses the effects of solvation on the reaction surface energetics of the β-lactamase active site model presented here (model 2). Specifically, single-point continuum solvation calculations at the RHF/6-31+G(d) level were performed for each stationary point on the surface using an asymmetric cavity defined by the isodensity surface at a value of 0.01. A value of 80, that for pure water, was chosen for the continuum dielectric constant. The following values for ΔE_e°(solv) were obtained for the five stationary points on the reaction surface, **R**, **PTTS1**, **I**, **PTTS2**, **P**: 0.00, 42.48, 25.78, 42.05, −20.39 kcal mol^{-1}. The results from such an approach should only be considered an upper bound to the effects of the complete environment, since the protein component of the environment certainly has a lower dielectric constant than 80.

Comparing these results with those in Table 1 shows that in all cases the relative energy is lowered with the solvent continuum included. As expected, the solvent continuum had the largest effect on the intermediate state where charge separation was most significant. The solvent caused only a slight reduction in the two proton-transfer transition states and had almost no effect on the relative energy of the product state. These results were found to parallel the change in dipole moment as the reaction system proceeds from reactants to products. A more detailed analysis of the effects of the protein environment are currently underway.

Acknowledgment. This research was supported by an award from Research Corporation.

JA963678G